Songklanakarin J. Sci. Technol.
42 (6), 1344-1351, Nov. - Dec. 2020

http://www.sjst.psu.ac.th

Original Article

MASW and ERT for near-surface characterization at the Huai Hong Khrai Royal Development Study Center, Doi Saket, Chiang Mai, Thailand

Siriporn Chaisri[1*], Suwimon Udphuay[2], Niti Mankhemthong[2], Weerapan Srichan[2], Pitak Kempet[3], and Phrudth Jaroenjittichai[3]

[1] *Department of Physics and Materials Science, Faculty of Science, Chiang Mai University, Mueang, Chiang Mai, 50200 Thailand*

[2] *Department of Geological Sciences, Faculty of Science, Chiang Mai University, Mueang, Chiang Mai, 50200 Thailand*

[3] *National Astronomical Research Institute of Thailand, Mae Rim, Chiang Mai, 50180 Thailand*

Received: 21 May 2019; Revised: 6 September 2019; Accepted: 18 September 2019

Abstract

Preliminary investigation of subsurface properties by geophysical methods were carried out over the construction site of the 40 meters Thai National Radio Telescope (TNRT) facility planning by National Astronomical Research Institute of Thailand (NARIT) in the Huai Hong Khrai Royal Development Study Center, Doi Saket, Chiang Mai, Thailand. Multichannel analysis of surface waves (MASW) and electrical resistivity tomography (ERT) were utilized in mapping of Vs distribution to obtain information on ground stiffness and other supporting information on subsurface electrical resistivity, respectively. Results from data analysis showed that the topsoil was very dense with thickness irregularly varied from 5 meters to10 meters overlying the bedrock with high variation in stiffness caused by the different degrees of weathering. The information obtained led to the conclusion that the proposed TNRT facility construction site is in the category of site class B of which the ground stability is moderate and less vulnerable to earthquake damages.

Keywords: MASW, ERT, NARIT, shear-wave velocity, electrical resistivity

1. Introduction

In 2018, the National Astronomical Research Institute of Thailand (NARIT) planned to construct a 40 meters Thai National Radio Telescope (TNRT) facility in the area of Huai Hong Khrai Royal Development Study Center, Doi Saket, Chiang Mai, Thailand as shown in Figure 1a, where the red star indicates the approximate location of the construction site. As with every large construction project, preliminary information on near-surface characteristics, such as ground stiffness and subsurface structure, beneath the target area were required at the beginning of the project for planning and designing buildings to house heavyweight objects and for future development. Subsurface property such as ground stiffness is directly related to stability of the building structure and possibility degree of earthquake hazards due to the liquefaction effect, (Richart, Hall, & Woods, 1970), the amplification of earthquake motion in soft sediments, (Kanli *et al.*, 2006). These characteristics are directly related to elastic properties of the supporting ground which corresponds to seismic wave properties (Bullen, 1963) especially the S-wave velocity (Vs). Moreover, ground amplifications from

*Corresponding author
Email address: siriporn.chaisri@cmu.ac.th

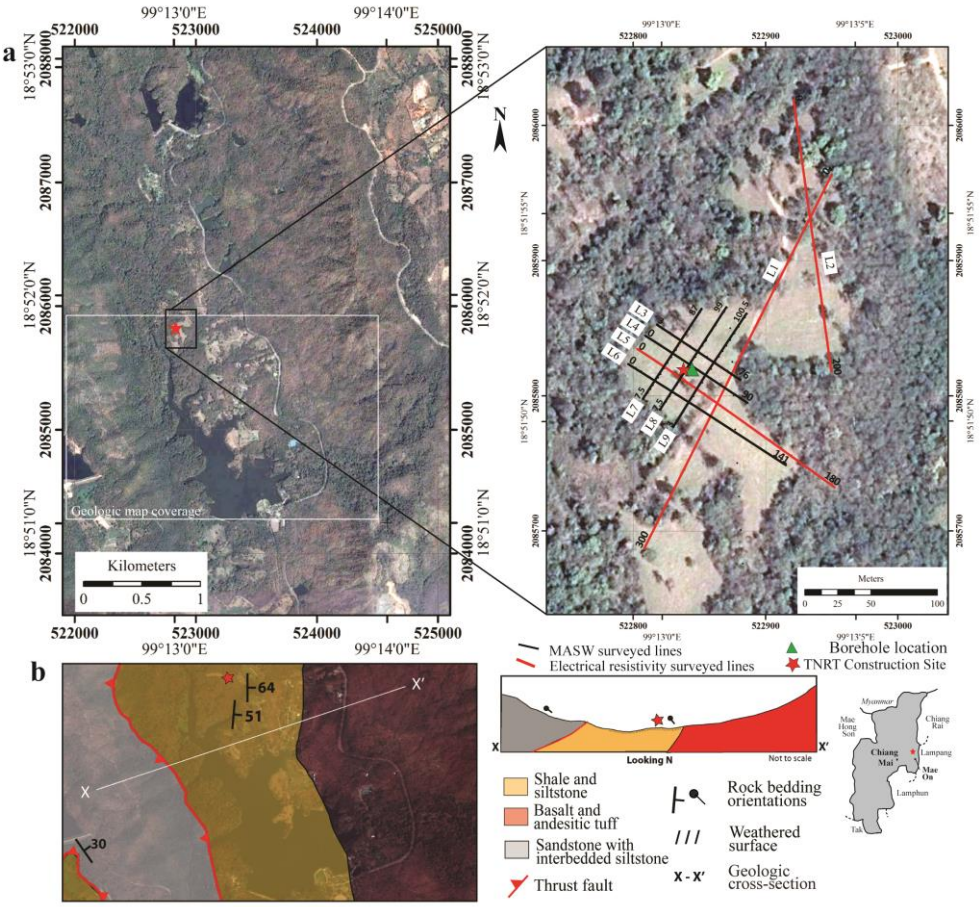

Figure 1. a) Map of geophysical surveys on the construction site of 40-m Thai National Radio Telescope (TNRT) facility plan-ning by National Astronomical Research Institute of Thailand (NARIT), Huai Hong Khrai Royal Development Study Center, Chiang Mai, Thailand. b) Geologic map showing the rock unit distributions and its geologic cross-section.

earthquakes depend on the subsurface properties in the upper 30 meters. The weighted average S-wave velocity in the upper 30 meters (Vs30m) is used as the seismic site characterization (SSC) classification to evaluate whether the construction site is safe against earthquakes. This classification is based on the recommendation of NEHRP (National Earthquake Hazards Reduction Program), BSSC (2009). It is also used as a crucial criterion in the design of building structures, smaller Vs30m subject to a larger ground amplification and suffer more damage from earthquakes. To evaluate Vs information, an application of seismic surface wave method, multichannel analysis of surface waves (MASW), was performed. In addition, electrical resistivity tomography (ERT) was also conducted to provide the supporting information on subsurface electrical resistivity. The final survey results from MASW and ERT of the TNRT construction site, shear-wave profile and electrical resistivity profile, were interpreted for identifying the bedrock and the thickness of topsoil layer.

2. Geologic Setting

The construction site is located approximately at an elevation of 385 meters in between high ridges flanking the western and eastern sides that are oriented in a north-south direction (Figure 1a). A geological survey covering about 6 square kilometers of the surrounding area (white rectangle in Figure 1a) indicates that the underneath rock units consist of coarse-grained sedimentary rocks (Mae Tha Formation) of thick-bedded sandstone interbedded with siltstone thrusting on fine-grained sedimentary rocks of shale and siltstone considered as the pelagic formation (Hara *et al.*, 2009) (Figure 1b). The pelagic formation rests on the volcanic formation of basalts, andesite, and andesitic tuffs which both formations are interpreted as typical ocean plate stratigraphy associated with a volcanic seamount, (Figure 1b) (Wakita & Metcalfe, 2005). The structural contacts of these rock units are shown in the schematic geologic map and cross-section (x-x´) in the right of Figure 1b. Based on the outcrop exposures found in this area along the tributary Huai Hong Krai on the south of the construction site (Figure 2a), the thickness of the topsoil or sedimentary layer overlaid the bedrock in the construction area should not be more than 5-10 meters. The hard bedrock below the topsoil is expected to be the fine-grained sedimentary rocks unit composed of highly deformed shale interbedded with thin-bedded siltstone that are mostly oriented in north-south direction tilted about 40 to 50 degrees to the east (Figure 2b).

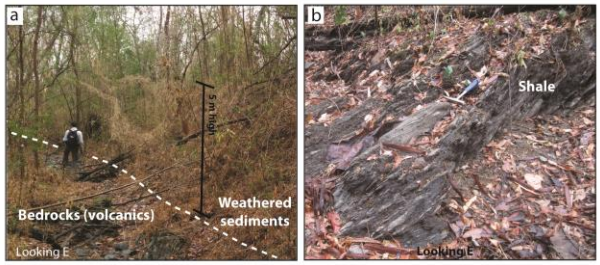

Figure 2. a) Photo of volcanic exposure along the tributary Huai Hong Krai showing the weathered sediment cover with an estimated thickness of 5 m. b) Photo of a fine-grained sedimentary rock unit composed of highly deformed shale interbedded with thin-bedded siltstone oriented in north-south direction with tilted about 40 to 50 degrees to the east.

3. Survey Methods

MASW and ERT techniques were employed in this study. There are 9 geophysical survey lines (Figure 1a right), three lines of ERT surveys, L1, L2 and L5, and eight lines of MASW surveys, excluding L1, as detailed in Table 1. The survey lines L2 and L5 were used in both techniques. The results from MASW of L3 to L9 were combined to create 3-dimensional image of Vs.

The key principle of MASW is based on the relationship between the phase velocity of surface wave and the depth range associated with wave motion, (Park, Miller, & Xia, 1999; Miller, Xia, Park, & Ivanov, 1999; Xia, Miller, & Park, 1999; Stokoe II, Wright, Bay, & Roesset, 1994). The velocity of surface wave for each frequency component (or phase velocity of surface wave) depends on the body wave velocity (P-wave and S-wave velocities) at the depth zone that corresponds with the wavelength of that wave frequency. It can be concluded that for stratified media such as soil-rock layers, surface waves will have dispersion property; phase velocities depending on wave frequencies. Therefore, if we detect the dispersion properties of surface waves, we can relate that to seismic body wave velocity especially S-wave velocity.

The main equipment for surface wave data acquisition is GeodeTM Exploration Seismograph, 24 channels per shot with 4.5 hertz geophones system and 20-pounds sledge-hammer for generating seismic waves. The common acquisition parameters had been tested base on the deepest target depth of 30 meters and optimum field parameters information from Park, Miller, & Miura (2002), to capture enough information on surface wave for analyzing. The common field acquisition parameters are 0.5 milliseconds of sampling interval, 1 second of total recording time, 4-5 times of shot stacking, and source offset varies from 2dx to 10dx, where dx is the receiver spacing. The survey lines L3 to L9 covered the TNRT construction area whereas L2 was aimed for future area development. Seismic data from field acquisition were processed with ParkSEIS© (v.2) for 2-D Vs profiles, Park Seismic LLC. (2018).

The spectrum of phase velocity created from seismic records is used as a tool for presenting the characteristic of surface wave dispersion (Park, Miller, & Xia, 1998), and then a dispersion curve of fundamental mode can be recognized and selected (Figure 3). Surface wave dispersion curve is the function of phase velocity related to the frequency of surface waves which will be inverted by a least-squares calculation method to determine the properties of earth layered media resulted in Vs as a function of depth. This Vs function represents the average S-wave velocities function in the middle of the geophone group in one shot of data acquisition. The whole set of field equipment is moved along the survey line for collecting data to the next location and then combine all solutions to create 2-D Vs profile visualizing the Vs cross section of soil-rock layer beneath the survey line.

ERT is a geo-physical technique for investigating the subsurface in terms of their electrical properties. The variations in electrical resistivity of the subsurface are characterized by variations in lithology, water/moisture content, porosity, permeability, and others. Such variations could be used to identify the sediment layer or soil layer, the high porosity and high moisture content corresponding to low electrical resistivity, and intact bedrock with low porosity and low moisture content corresponding to high electrical resistivity. ERT data acquisition requires the injection of electrical current into the ground through a pair of electrodes creating electrical potential field surround the area. By measuring the resulting potential field on the ground surface with several selected pairs of electrodes, the electrical resistivity values are recorded and a pseudo cross-section of apparent resistivity beneath the survey line can be

Table 1. Information of ERT and MASW surveys on 9 survey lines.

Survey	Dipole-Dipole ERT surveys		Surface wave - MASW surveys		
Line	Survey distance (m)	Electrode spacing (m)	Geophone spacing dx (m)	Survey distance (m)	2-D Vs profile (m)
L1	300	5	×	×	×
L2	200	5	2.5	177	120
L3	×	×	1.5	76	41
L4	×	×	1.5	90	56
L5	180	4.5	1.5	141	106
L6	×	×	1.5	141	106
L7	×	×	1.5	80	45
L8	×	×	1.5	91	57
L9	×	×	1.5	98	57

Note: symbol × indicates no survey was done.

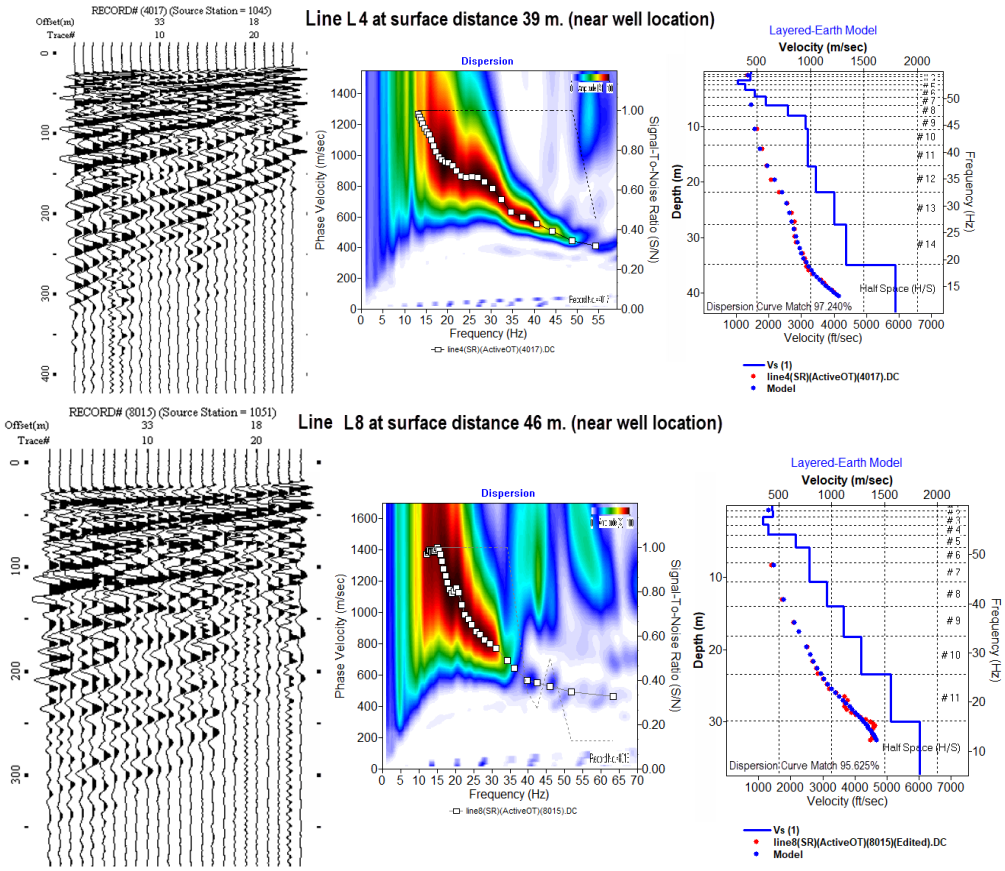

Figure 3. The example MASW shot records from survey line (Top) L4 and (Bottom) L8 at surface distance 39 meters and 46 meters, respectively; approximately at well location, and from left to right, shot record, dispersion curve selection, and final one-dimension Vs model, respectively.

made. The investigation depth of ERT depends on the geometry of measuring electrode pairs, the separation of current and potential electrodes. The larger electrode distances correspond to the measurement in the greater depths, (Everett, 2013; Loke, 2018).

Three survey lines of 2D ERT data were collected using ABEM TERRAMETER SAS4000 resistivity meter with four cables of ES10-64C electrode selector. The dipole-dipole electrode configuration was used with minimum electrode spacing of 4.5 and 5 meters as indicated in Table 1. The apparent resistivity data were inverted by a finite-difference algorithm using RES2DINV software to obtain the true electrical resistivity cross-section model.

4. Survey Results

Subsurface layers were classified by information from Vs and electrical resistivity corresponding to results from the geological survey and rock types found in the area (Figure 2). There was also borehole data available from NARIT internal soil report (SIS instruments, 2018). The borehole was located in the middle of the construction site marked as a green triangle on the survey map in Figure 1 closed to the crossing of survey lines L4 and L8 with maximum drilling depth of 13.5 meters. Logging information was grouped in 3 zones depending on their physical properties: 0-3 meters was clayey sand sediment with increasing soil stiffness, 3-10.43 meters was high stiff sandy clay with trace of some rock fragment that might come from decomposed shale, and 10.43-13.5 meters was moderately weathered calcareous shale with bed dipping of 45 degrees. Therefore, it may be concluded that a topsoil layer ranged from clayey sand to sandy clay from the decomposed shale bedrock whereas the bedrock underneath a topsoil layer was shale and siltstone with interbedded sandstone. This conclusion was strongly supported by information obtained from the geological survey, rock samples and outcrops (Figure 1 and Figure 2), with moderate weathering at the upper zone.

The results from both methods, presented with color contour cross-sections, revealed variations in the corresponding subsurface properties which, in turn, enabled identification of boundaries between different lithologies. From MASW surveys, lines L2, L3 and L4 have approximately 30 dispersion curves, L5 and L6 have approximately 75 dispersion curves, and L8 and L9 have approximately 40 dispersion curves to analyze with maximum 30 meters investigation depth. Figure 3 shows the selected shots from L4 and L8, where the midpoints of their geophone groups are approximately close to well position. Shot record was map into the phase velocity spectrum for dispersion curve extraction and

then inverse calculation were done, resulted in one-dimensional Vs model. All the solutions from MASW were combined and the outputs yield 2-D S-wave velocity cross sections (Figure 4). The results can be interpreted with three possible distinct lithologies, topsoil, soft bedrock or weathered bedrock zone, and hard or fresh bedrock zone in the deeper part. The contact between topsoil and bedrock, indicated by dash line with Vs=600 meter/second and that between soft and hard bedrock was indicated by black solid line with Vs=1100 m/sec. From ERT surveys, the outputs yield 2-D electrical resistivity cross sections (Figure 5) with the deepest depth about 60, 20, and 40 meters on lines L1, L2 and L5, respectively. On resistivity model, the contact between topsoil and bedrock indicated by dash line define 100 ohm.meter. According to the model, resistivity values of less than 100 ohm.m shows the possibility of topsoil layer and that greater than 100 ohm.meter shows the possibility of bedrock. The topsoil layer has a low value of Vs and resistivity, S-wave velocity ranging from 250-600 meter/second with resistivity less than 100 ohm.m, and approximately 5-10 meters thick (Figure 5). Bedrock has a high value of Vs and resistivity, S-wave velocity greater than 600 meter/second with resistivity values of more than 100 ohm.meter. The 2-D Vs profiles resulting from the survey lines L3 to L9 are combined to generate 3-D Vs volume for creating the interface between layers (Figure 6), Vs 600 meter/second surface indicates the bottom of topsoil layer or the top of bedrock and Vs 1,100 meter/second surface indicates weathering bedrock zone and fresh bedrock interface. The bedrock surface shows unevenly depth range between 5 to 10 meters with irregular weathering zone, consistent with resistivity cross sections (Figure 5). The topsoil layer is hard and dense sandy clay from the

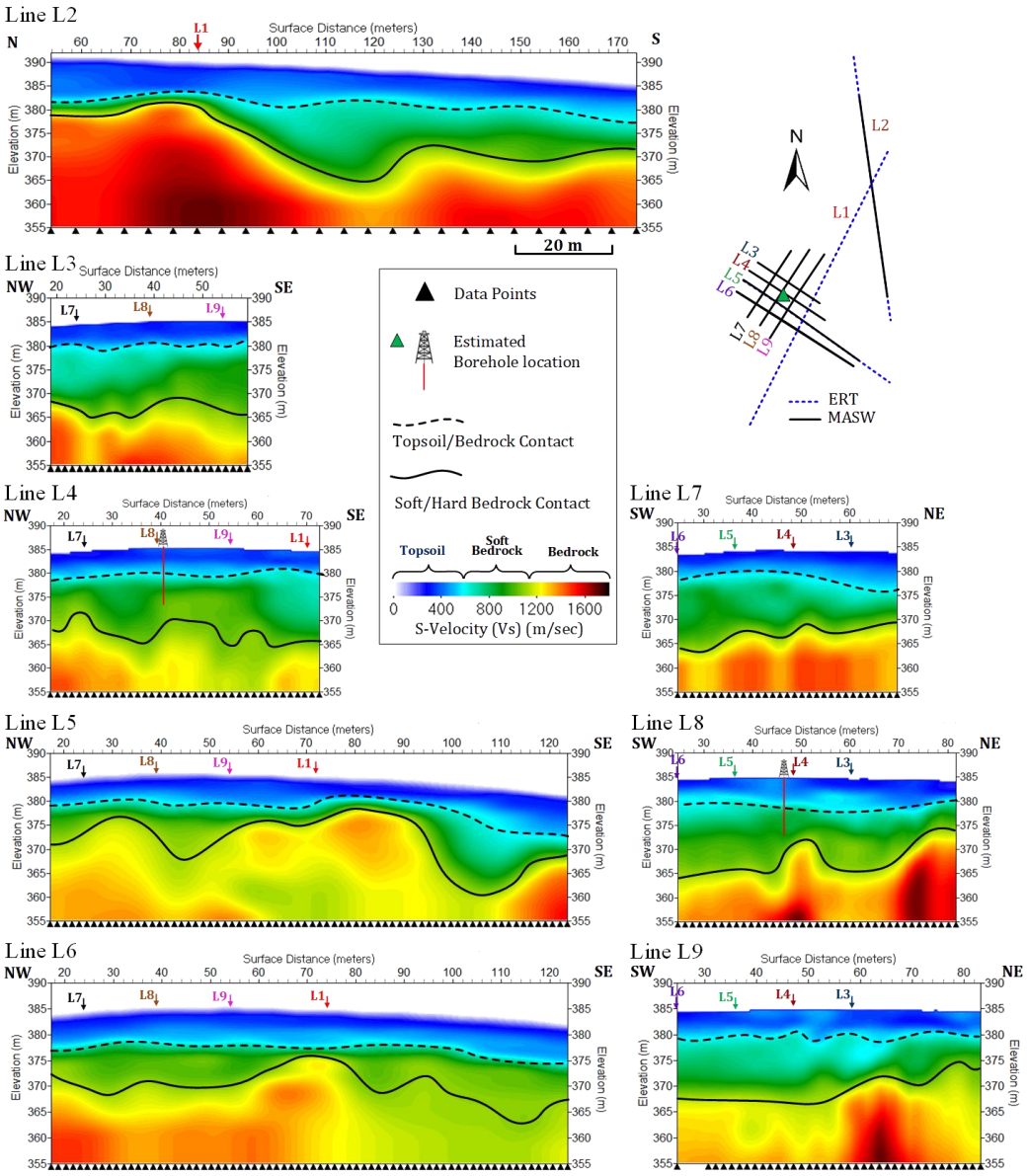

Figure 4. Results from MASW show 8 of S-wave velocity cross section from L2 to L9 with the same horizontal distance scale and color contour. The borehole is located near the crossing of L4 and L8.

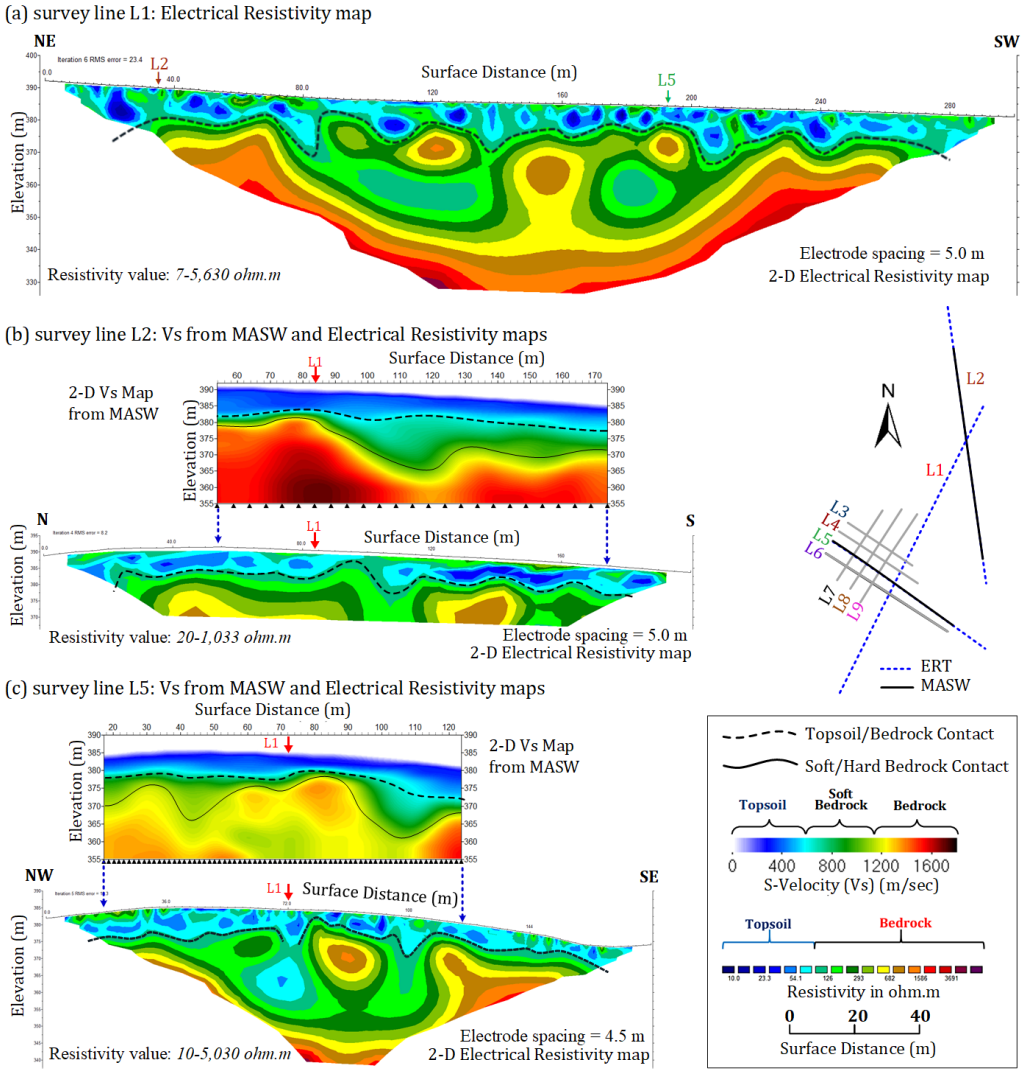

Figure 5. (a) Electrical resistivity profile from survey line L1, and that with 2-D Vs profiles from MASW (b) L2 and (c) L5.

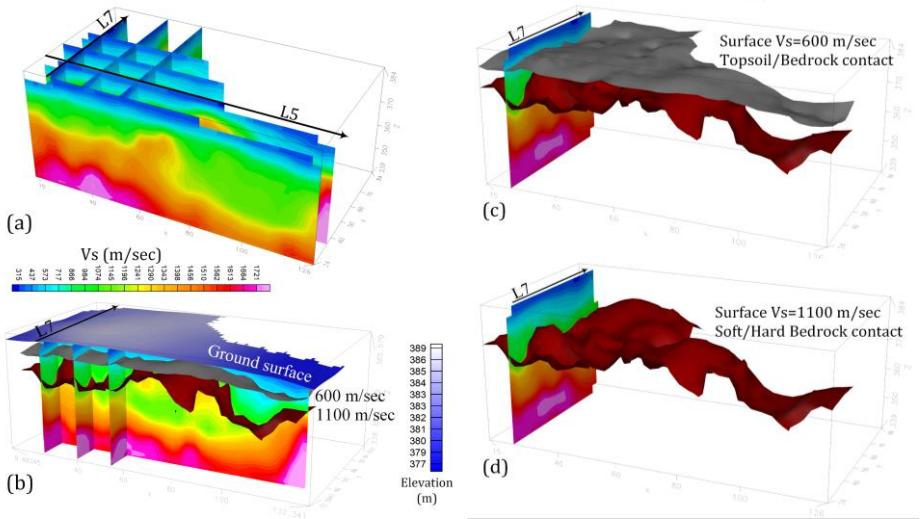

Figure 6. 3-D Vs volume from MASW creating interface between layers, Vs 600 m/sec surface is the top of bedrock and Vs 1,100 m/sec surface is weathered bedrock and fresh bedrock interface.

decomposed shale bedrock. Moreover, the Vs30m evaluated from survey line L5 and L6 are 770 m/sec and 783 m/sec which corresponding to the seismic site classification class B, (Figure 7), classify the study area as a rock type with moderate fracturing and weathering. This is meaning that the construction site has moderate ground stability, less affected by earthquakes.

5. Discussion

The results showed that the value of S-wave velocity of the topsoil at the construction site ranged between 250 to 600 meter/second indicated stiff and very dense topsoil, whereas that of the bedrock ranged from 600 to 1600 meter/second indicating high variation in stiffness that may be caused by different degrees of weathering. From the geological survey and logging information, the bedrock is shale interbedded with sandstone tilted orientation 45 degrees. The sandstone part of the bedrock has higher durability and thus slower erosional rate than that of the shale. The erosion process could create fractures on rock surface that allows penetration of water or other solutions, therefore, in weathering zone the medium will be less dense and become more electrically conductive, low resistivity. Because of the tilted orientation of the bedrock, the top of the bedrock underwent different erosional rates resulted in un-evenly surface as seen in Figure 6, Vs 600 meter/second and Vs 1100 meter/second surfaces. This also affected the thickness of the topsoil sediment layer, irregularly varied from 5-10 meters indicated by the color zone of electrical resistivity less than 100 ohm.m and Vs less than 600 meter/second. Although, the hard bedrock has irregular depth and high variation in stiffness, the overall of the site can be characterized by moderate to high Vs30m value. The construction site is situated on the dense soil sediment underlain by the bedrock layer with high stiffness indicated that the less effect of ground amplifications from earthquakes. The knowledge of soil stiffness which express in the form of S-wave velocity obtained from this study is helpful for estimating ground response at construction sites by the engineer, and now, the TNRT is under construction and schedules to be completed by the year 2020.

6. Conclusions

Preliminary characteristics of subsurface properties in terms of S-wave velocity and electrical resistivity, related to subsurface stiffness, were obtained from geophysical survey data employing the MASW and ERT methods. The results were consistent with information obtained from borehole logging data. This supported our analysis of Vs distribution covering the construction area. The electrical resistivity values of the topsoil were less than 100 ohm-m with Vs less than 600 m/sec. This may be interpreted that the topsoil layer is very dense with irregular thickness ranged from 5-10 meters. The electrical resistivity which is more than 100 ohm.meter and the Vs range of 600-1600 meter/second of the bedrock show that there is a large variation of the stiffness. From the average shear wave velocity value, Vs30m, obtained in seismic site characterization, it may be stated that the construction site of a 40 meters TNRT facility is classified as site class B, identified by rocks with moderate fracturing and weathering structures. The ground stability at the site is moderate with less effect from earthquake damages.

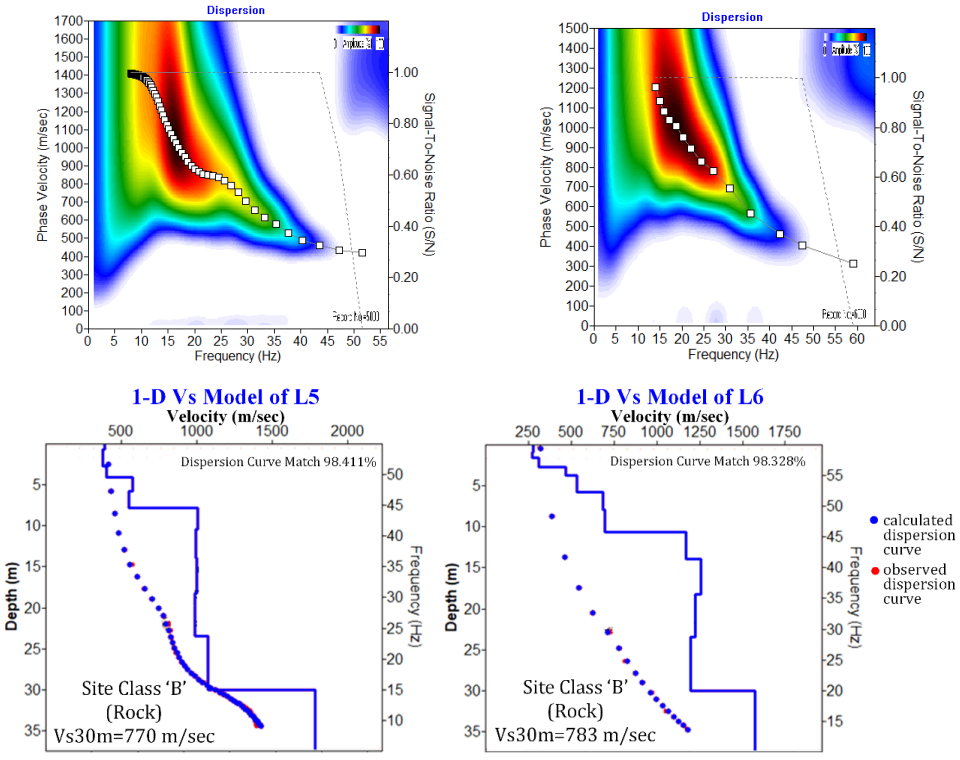

Figure 7. Seismic site classification indicates the site as Class B, blue line is the final Vs model for Vs30m evaluation.

Acknowledgements

All authors thank the National Astronomical Research Institute of Thailand (NARIT) for the financial support and borehole logging data. Further thanks to the Huai Hong Khrai Royal Development Study Center for the permission to conduct the surveys. This work could not be completed without help from the staff of Geophysics Research Laboratory, Department of Geological Sciences, Faculty of Science, Chiang Mai University, for their support in fieldwork and data discussion. This paper was a poster presentation at the 8th International Conference on Applied Geophysics, November 8-10, 2018, Songkhla, Thailand, and selected by the conference scientific committee for publication.

References

BSSC. (2003). *NEHRP recommended provision for seismic regulation for new buildings and other structures (FEMA 450), Part 1: Provisions.* Washington, DC: Building Safety seismic council for the federal Emergency Management Agency.

Bullen, K. E. (1963). *An introduction to the theory of seismology*. New York, NY: Cambridge University Press.

Everett, M. E. (2013). *Near-surface applied geophysics*. New York, NY: Cambridge University Press.

Hara, H., Wakita K., Ueno, K., Kamata, Y., Hisada, K., Charusiri, P., . . . Chaodumrong, P. (2009). Nature of accretion related to Paleo-Tethys subduction recorded in northern Thailand: Constraints from mélange kinematics and illite crystallinity. *Gondwana Research*, *16*, 310-320.

Kanli, A. I., Tildy, P., Pronay, Z., Pinar, A., & Hemann, L. (2006). Vs30 mapping and soil classification for seismic site effect evaluation in Dinar region, SW Turkey. *Geophysical Journal International*, *165*, 223–235.

Loke, M. H. (2018). *Tutorial: 2-D and 3-D electrical imaging surveys*. Retrieved from http://www.geotomosoft.com. [Oct 5, 2018].

Miller, R. D., Xia, J., Park, C. B., & Ivanov, J. M. (1999). Multichannel analysis of surface waves to map bedrock, Kansas Geological Survey. *The Leading Edge*, *18*, 1392-1396.

Park, C. B., Miller, R. D., & Miura, H. (2002). *Optimum field parameters of an MASW survey, Expanded Abstract.* Tokyo, Japan: SEG-J.

Park Seismic LLC. (2018). *Multichannel analysis of surface waves*. Retrieved from http://www.masw.com.

Park, C. B., Miller, R. D., & Xia, J. (1998). Imaging dispersion curves of surface waves on multi-channel record. *The 68th Annual International Meeting Society of Exploration Geophysicists, Expanded Abstracts*, 1377-1380.

Park, C. B., Miller, R. D., & Xia, J. (1999). Multichannel analysis of surface waves. *Geophysics*, *64*, 800-808.

Richart, F. E., Hall, J. R., & Woods, R. D. (1970). *Vibrations of soils and foundations*. Upper Saddle River, NJ: Prentice-Hall.

SIS Instruments, Co., Ltd. (2018). *Soil report on the construction site of the 40-m Thai National Radio Telescope (TNRT), Huai Hong Khrai Royal Development Study Center, Doi Saket, Chiang Mai* (Internal report of the National Astronomical Research Institute of Thailand: Unpublished).

Stokoe II, K. H., Wright, S. G., Bay, J. A., & Roesset, J. M., (1994). *Characterization of geotechnical sites by SASW method, in Geophysical characterization of sites. ISSMFE Technical Committee #10*, New Delhi, India: Oxford.

Wakita, K., & Metcalfe, I. (2005). Ocean plate stratigraphy in East and Southeast Asia. *Journal of Asian Earth Sciences*, *24*, 679–702.

Xia, J., Miller, R. D., & Park, C. B. (1999). Estimation of near-surface shear-wave velocity by inversion of Rayleigh wave. *Geophysics*, *64*, 691-700.